Measurement of force acting on a moving part of a pneumatic linear bearing

Yusaku Fujii[a)]
Faculty of Engineering, Department of Electronic Engineering, Gunma University, 1-5-1 Tenjin-cho, Kiryu 376-8515, Japan

(Received 27 December 2002; accepted 17 March 2003)

A method for evaluating the components of the force acting on a moving part of a pneumatic linear bearing is proposed. The total force acting on the moving part is accurately measured as the inertial force using an optical interferometer. Then, the components of the force, such as the force component depending on position, the force component depending on velocity, and the force component depending on tilt angle, are evaluated using the least-squares method. In the experiment, the total force acting on the moving part is measured with the standard uncertainty of approximately 0.001 N, which corresponds to approximately 0.003% (30 ppm) of the gravitational force acting on it ($\mathbf{M}=4.119$ kg) of approximately 40 N (40 N). The experimentally evaluated values of these force components well coincide with the theoretically expected values. © *2003 American Institute of Physics.* [DOI: 10.1063/1.1574396]

I. INTRODUCTION

Pneumatic linear bearings have the two major features, i.e., high accuracy in motion and low friction. For the former feature, these bearings are widely used in various precision instruments[1–3] in which precise linear motion is required. There has been some research concerning this feature.[4,5]

For the latter feature, the author uses these bearings in the research on methods for measuring mass under weightless conditions[6] and for evaluating the impulse response of force transducers,[7,8] in which we require a linear bearing with low friction. However, there are some ambiguous points about the force acting on the moving parts of a pneumatic linear bearing.

In our previous research,[9] the frictional characteristics of a pneumatic linear bearing were roughly investigated. In this work, the total force acting on the moving part is accurately measured as the inertial force using an optical interferometer. Then, the components of the force, such as the force component depending on position, the force component depending on velocity, and the force component depending on tilt angle, are evaluated using the least-squares method.

II. EXPERIMENTAL SETUP

Figure 1 shows the experimental setup for measuring the force acting on the moving part of a linear bearing. In the experiment, the initial velocity of the moving part is given to the moving part by hand, in other words, manually. Then, the moving part begins to move back and forth between the two dampers. The velocity of the moving part is accurately measured using an optical interferometer and electric frequency counters.

The total force acting on the moving part is measured as the product of mass and acceleration, $\boldsymbol{\alpha}$ (m/s^2). The acceleration is calculated by differentiating the velocity, $\mathbf{v}$ (m/s), with respect to time. The velocity is measured as the Doppler shift frequency of the signal beam of a laser interferometer, f_{Doppler}, which can be expressed as

$$\mathbf{v}=\lambda_{\mathrm{air}}(f_{\mathrm{Doppler}})/2,$$

$$f_{\mathrm{Doppler}}=-(f_{\mathrm{beat}}-f_{\mathrm{rest}}),$$

where λ_{air} is the wavelength of the signal beam under the experimental conditions; f_{beat} is the beat frequency, which is the frequency difference between the signal beam and the reference beam; and f_{rest} is the rest frequency, which is the value of f_{beat} when the moving part is at a standstill. The direction of the coordinate system for the position, velocity, acceleration, and force acting on the moving part is set to be towards the right in Fig. 1.

A Zeeman-type two-frequency He–Ne laser is used as the light source. The frequency difference between the signal beam and the reference beam, i.e., the beat frequency, f_{beat}, is measured from an interference fringe that appears at the output port of the interferometer; which varied around f_{rest}, approximately 2.6 MHz, depending on the velocity of movement. An electric frequency counter (model: R5363; manufactured by Advantest Corp., Japan) continuously measures and memorizes the beat frequency, f_{beat} (Hz), 1000 times with a sampling interval of $T=40\,000/f_{\mathrm{beat}}$ (s). In other words, it continuously measures the time of every 40 000 periods without dead time, calculates the frequency; and stores the 1000 values in memory. The sampling period of the counter is approximately 15 ms at the frequency of 2.6 MHz. Another electric counter (model TA1100, manufactured by Yokogawa Corp., Japan) measures the rest frequency, f_{rest} (Hz), using an electric signal supplied by a photodiode embedded inside the He–Ne laser.

Measurement of the electric counter (R5363) is triggered by means of a light switch, i.e., a combination of a laser

[a)]Electronic mail: fujii@el.gunma-u.ac.jp

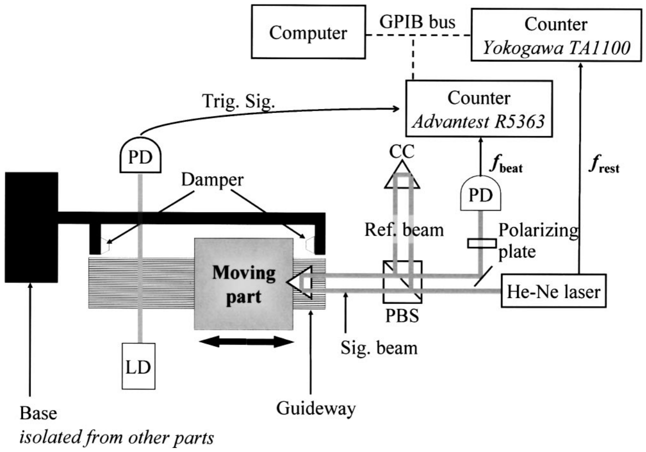

FIG. 1. Experimental setup.

diode and photodiode. The total mass of the moving part, including the cube corner prism, is approximately 4.119 kg.

Figure 2 shows the angle measurement system. A linear bearing is mounted on a tilting stage whose tilt angle is adjustable. The angle of the stage is measured by an autocollimator (model ELCOMAT 2000, manufactured by Moeller-Wedel Optical, GmbH, Germany) with the resolution of 0.05 s, i.e., approximately 0.25 μrad. The origin of the autocollimator is roughly set so that the moving part is at a standstill at the center of the guideway.

Figure 3 shows the schematic of the pneumatic linear bearing, ''Air-Slide TAAG10A-01'' (NTN Co., Ltd., Japan). The compressed air supplied from outside is first introduced into the guideway rather than directly into the moving part. The reason for this is to avoid pressure piping on the moving part. Then, air comes out from air outlets at the center of the guideway, and introduced into the air inlets at the center of the moving part through the air passage channels grooved on the inner surface of the moving part along the direction of motion. In the design, airflow between the guideway and the moving part is always bilaterally symmetric except in the air passage channels. This is for suppressing the static force acting on the moving part. The stroke of the moving part is approximately 100 mm, the maximum weight of the moving part is approximately 30 kg, the thickness of the air film without weight is approximately 8 μm, the stiffness of the air film is approximately 80 N/μm, and the straightness of the guideway surface is approximately 0.1 μm/100 mm.

The angle of the guideway, at which the moving part is at a standstill, changes according to the position of the moving part. A static force, whose direction is toward the center and whose magnitude increases as the distance increases, seems to exist. The pressure difference between the two sides of the air passage channels shown in Fig. 3, which changes according to the relative position of the air outlets on the guideway and the air inlets on the moving part, is a possible cause of this static force.[9] The sidewalls of the air passage channels closer to the air outlet will be at a higher pressure than the farther sidewalls because of the pressure loss along the air passage channels. This results in the static force acting on the moving part toward the center.

III. MEASUREMENT

In the experiment, three sets of measurement are conducted against five values of the stage angle, i.e., −0.6, −0.3, 0.0, 0.3, and 0.6 mrad. In each set, the beat frequency for more than three reciprocating motions was measured.

Figure 4 shows the data processing procedure of calculating the velocity, position, acceleration, and force from the frequency. In the experiment, only the beat frequency, f_{beat}, and the rest frequency, f_{rest}, are measured using the optical interferometer and the electric counters. The velocity, **v**; position, **x**; acceleration, $\boldsymbol{\alpha}$; and force, **F**, are calculated from the beat frequency, f_{beat}, and the rest frequency, f_{rest}. In the case shown in Fig. 4, the stage angle is 0.0 mrad. During collision of the moving part with the dampers, the frequency and the velocity change suddenly and sharp pulses appear in the acceleration and force. The origin of the position, **x**, is set to be the center of the traveling section of the moving part.

Figure 5 shows the result of the same measurement as Fig. 4, but in a different manner. This is the enlarged view of the figure on the force in Fig. 4. In Fig. 5, all measured data and the selected data are shown. The selected data are chosen under the condition that the moving part is apart from the dampers more than 5 mm and the motion is in the first three sets of reciprocating motion.

Figure 6 shows the distribution of the measured force, **F** (N), of all the 15 measurements against the time, **T** (s), the position, **x** (m), the velocity, **v** (m/s), and the tilt angle of the stage, θ (mrad). All 6859 sets of data, which consist of the measured values of **F** (N), **T** (s), **x** (m), **v** (m/s), and θ (mrad), are plotted in Fig. 6. Mutual relationships of the

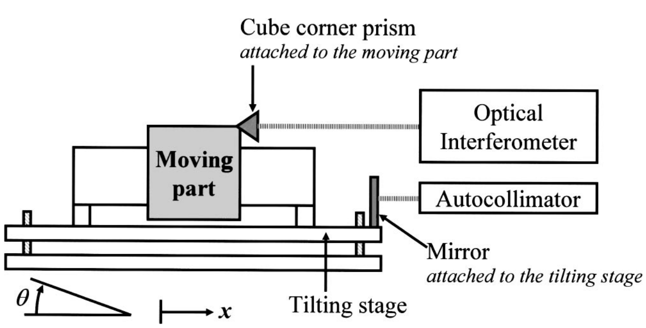

FIG. 2. Angle measurement system.

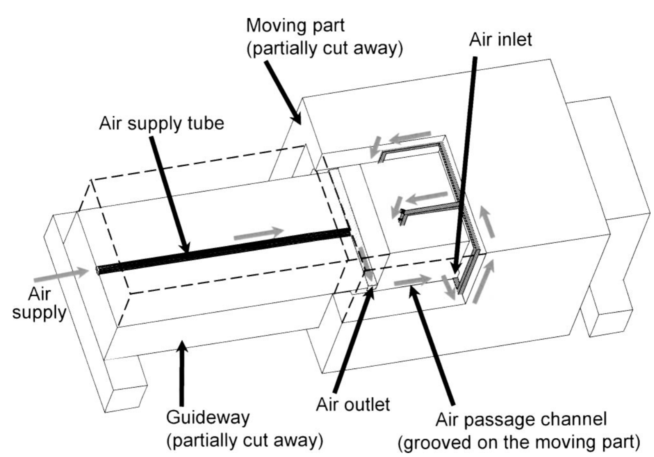

FIG. 3. Schematic of the linear bearing.

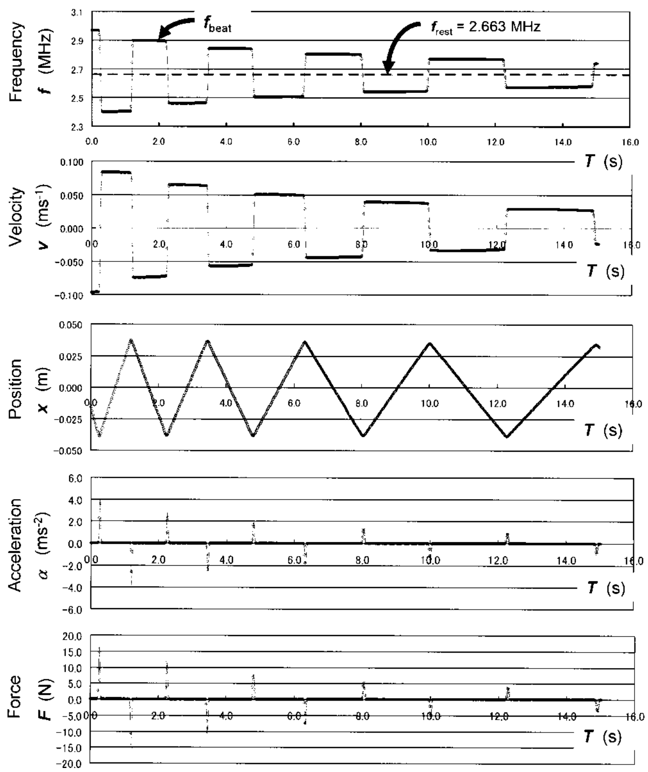

FIG. 4. Data processing: from frequency to velocity, position, acceleration, and force (tilt angle of the guide way $\theta = 0.0$ mrad; mass of the moving part $\mathbf{M} = 4.119$ kg).

force against the position, the velocity, and the tilt angle of the stage are sufficiently estimated from Fig. 6. The coefficients of correlation of the force against the position, velocity, and tilt angle of the stage are observed to be negative, negative, and positive, respectively.

IV. REGRESSION ANALYSIS

Under the assumption that the force acting on the moving part is the sum of the components in proportion to the position, velocity, and tilt angle, the following is derived:

$$\mathbf{F} = A_1\mathbf{x} + A_2\mathbf{v} + A_3\theta + A_4.$$

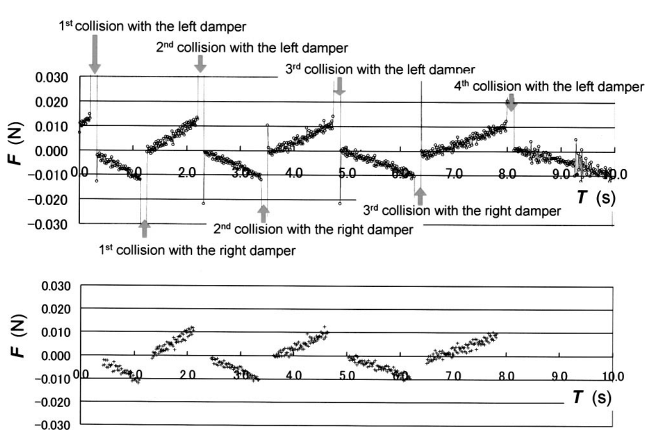

FIG. 5. Inertial force acting on the moving part of the bearing: (a) all obtained data and (b) selected data for analysis (first three sets of reciprocating motion, $-38\ \text{mm} < X < 38\ \text{mm}$).

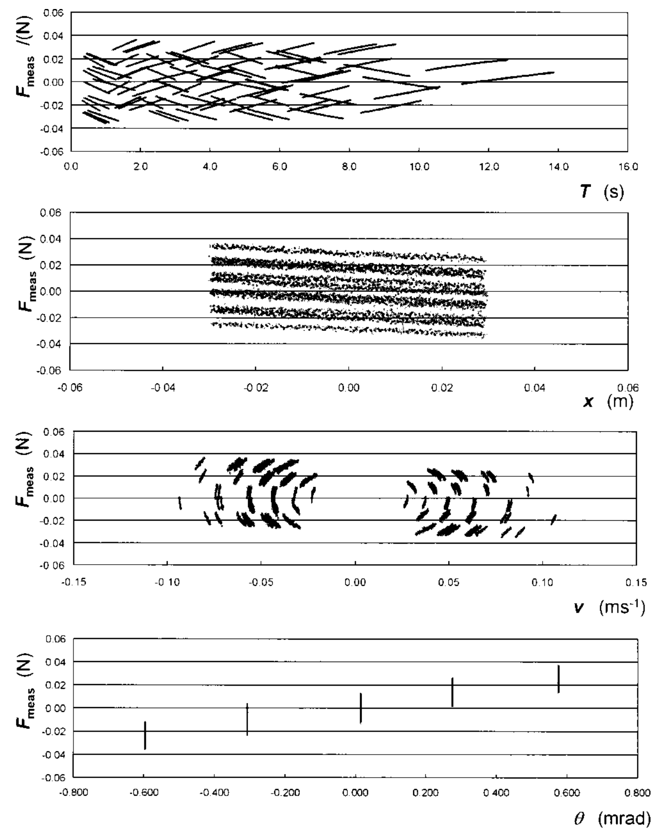

FIG. 6. Distributions of the measured force against the time, position, velocity, and tilt angle of the guideway.

Using the 6859 sets of data (Fig. 6), the four coefficients of the equation, A_1, A_2, A_3, and A_4, are determined by means of the least-squares method.

Table I shows the coefficients obtained experimentally and theoretically. The experimental results are obtained by means of the least-squares method. On the other hand, the theoretical estimates are derived as follows:

A. Theoretical estimate of A_1

The coefficient, A_1, corresponds to the force component being proportional to the position of the moving part, which was measured to be -1.5×10^{-1} (N/m) in the static condition.[9] This is thought to come from the pressure difference between the two sides, i.e., the right and left sidewalls, of the air passage channels shown in Fig. 3, as explained above. Under the assumption that this static force acts as it is even when the moving part is in motion, the value of the theoretical estimate is -1.5×10^{-1} (N/m). The difference between the experimental results and the theoretical estimate is approximately 0.2×10^{-1} (N/m).

TABLE I. Coefficients obtained experimentally and theoretically.

	Experimental results (results of regression)	Theoretical estimates
A_1 (N/m)	-1.7×10^{-1}	-1.5×10^{-1}
A_2 (N/ms^{-1})	-8.2×10^{-2}	-5.9×10^{-2}
A_3 (N/rad)	4.2×10^{1}	4.0×10^{1}
A_4 (N)	6.6×10^{-4}	0

B. Theoretical estimate of A_2

The coefficient A_2 is thought to correspond to the dynamic frictional force acting on the moving part, $\mathbf{F}_D$. Under the assumption that the dynamic frictional force is equal to the frictional drag of Couette flow in the air film, it is expressed as

$$\mathbf{F}_D = -\mu_{air}\mathbf{S}/\mathbf{h}\mathbf{v} = A_2\mathbf{v},$$

where μ_{air} is the coefficient of viscosity of air, $\mathbf{S}$ is the surface area of the inside wall of the moving part that is in contact with the air film, $\mathbf{v}$ is the velocity of the moving part, and $\mathbf{h}$ is the thickness of the air film. Then, the dynamic frictional force, $\mathbf{F}_D$, is proportional to the velocity of the moving part, $\mathbf{v}$. The coefficient A_2 is calculated to be -5.9×10^{-2} (N/ms^{-1}) using the nominal value of the thickness, $\mathbf{h}$, of approximately 8 μm. The difference between the experimental results and the theoretical estimate of approximately 0.23×10^{-2} (N/ms^{-1}) is thought to come from the form tolerance of the air–film formed by the outer shape of the guideway and the inner shape of the moving part.

C. Theoretical estimate of A_3

The coefficient A_3 is thought to correspond to the component of the force of gravitation in the direction of the guideway, and it is expressed as

$$\mathbf{F} = \mathbf{Mg}\sin\theta = \mathbf{Mg}\,\theta = A_3\,\theta,$$

where $\mathbf{M}$ is the mass of the moving part of, approximately, 4.119 kg; $\mathbf{g}$ is the acceleration due to gravity; and θ is small enough. Therefore, the coefficient A_3 is calculated to be 4.0×10^1 (N/rad). The difference between the experimental results and the theoretical estimate is approximately 0.2×10^1 (N/rad).

D. Theoretical estimate of A_4

The coefficient A_4 is zero in the ideal conditions. The experimental result of approximately 6.6×10^{-4} (N) is small enough to be ignored.

As shown above, the experimental results well agree with the theoretical estimates (Table I). This indicates both the accuracy of the force measurement and the validity of the supposed form of regression equation.

Figure 7 shows relationship between the measured force, $\mathbf{F}_{meas}$ (N), and the calculated force using the above expression, $\mathbf{F}_{cal}$ (N). The root-mean-square value of the difference between $\mathbf{F}_{meas}$ and $\mathbf{F}_{cal}$ is 0.0016 N (1.6 mN). This corresponds to, approximately, 4% of the maximum measured force of, approximately, 0.04 N (40 mN). This also indicates both the accuracy of the force measurement and the validity of the supposed form of the regression equation.

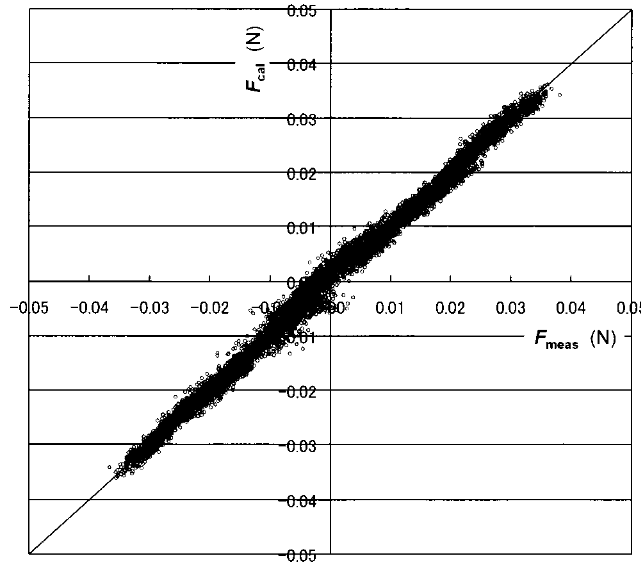

FIG. 7. Relationship between the measured force and the calculated value using the regression equation.

V. DISCUSSION

To evaluate the uncertainty in measuring force acting on the moving part, the force was measured under the condition that the moving part is fixed to the upper plate of the tilting stage using a rubber plate. The measurement procedure is the same as shown above (Fig. 4). If the moving part is at a standstill and the measurement uncertainty can be negligible, the measured force should be zero. Actually, the root-mean-square value of the measured force was approximately 0.0011 N (1.1 mN). Under the condition that the moving part is in motion, the measurement uncertainty is thought to be almost the same. Therefore, the uncertainty in measuring the force shown in Fig. 6 is estimated to be approximately 0.001 N (1 mN). This corresponds to, approximately, 3% of the maximum measured force of approximately 0.04 N (40 mN). This also corresponds to, approximately, 0.003% (30 ppm) of the gravitational force acting on the moving part ($\mathbf{M}$ = 4.119 kg) of approximately 40 N.

As for that the root-mean-square value of the difference between $\mathbf{F}_{meas}$ and $\mathbf{F}_{cal}$ was 0.0016 N (1.6 mN), this is slightly larger than the measurement uncertainty of 0.001 N (1 mN). The following are the conceivable causes for this:

(a) Some unknown components of force, which are not considered in the used regression equation, exist.

(b) The force acting on the moving part in motion actually varies because of the accidental change of the state of the airflow inside the bearing.

Using this method, the force acting on the moving part of a linear bearing can be accurately measured, and the validity of arbitrary regression equations can be determined. This method will be effective to elucidate the generation mechanism of the force acting inside the linear bearing.

The total time, which is required for conducting all the experiments and analyses shown in the experiment, is less than 1 h, once the experimental setup is prepared. Therefore, this method will also be convenient for inspecting the profile quality of bearings in the manufacturing process.

ACKNOWLEDGMENTS

The author thanks Y. Nakamura and N. Hamaya at Gunma University for their technical help in the experiment.

[1] M. Negishi, A. Deguchi, M. Ando, M. Takimoto, and N. Nakamura, Nanotechnology **6**, 139 (1995).
[2] S. Hosoe and T. Yoshida, Nanotechnology **4**, 206 (1993).
[3] H. Onda, A. Asahara, and S. Fujii, JSPE **58**, 1837 (1992) (in Japanese).
[4] T. Egami and T. Nishiyama, Trans. Soc. Instrum. Control Eng. (Japan) **30**, 118 (1994) (in Japanese).
[5] I. Watanabe, H. Aoyama, and A. Shimokohbe, JSPE **54**, 329 (1988) (in Japanese).
[6] Y. Fujii, H. Fujimoto, R. Watanabe, and Y. Miki, AIAA J. **39**, 455 (2001).
[7] Y. Fujii, Metrologia **38**, 83 (2001).
[8] Y. Fujii, Meas. Sci. Technol. **14**, 65 (2003).
[9] Y. Fujii and H. Fujimoto, Meas. Sci. Technol. **10**, 362 (1999).